Computational Study of the Effect of the Imidazole Ring Orientation on the EPR Parameters for Vanadyl−Imidazole Complexes

Alexander C. Saladino and Sarah C. Larsen*

Department of Chemistry, University of Iowa, Iowa City, Iowa 52242

Received: June 28, 2002; In Final Form: August 29, 2002

The vanadium hyperfine coupling constant for vanadyl−imidazole complexes depends on the orientation of the imidazole ring with respect to the vanadyl bond as illustrated by a recent electron paramagnetic resonance (EPR) study of vanadyl−imidazole model complexes (Pecoraro, et al. *J. Am. Chem. Soc.* **2000**, *122*, 767). In the study reported here, density functional theory (DFT) calculations of EPR hyperfine and quadrupole coupling constants for a model complex, $[VO(imid)(H_2O)_4]^{2+}$, were used to elucidate the orientation dependence of the vanadium and nitrogen hyperfine coupling constants for an equatorially coordinated imidazole ligand. The computational results for the orientation dependence of the vanadium hyperfine coupling constant reproduce the functional dependence ($A_{||}$(imidazole) $= A + B \sin(2\theta - 90)$) observed in the experimental EPR data. The computational results predict similar orientation dependence for the vanadium quadrupole coupling constant and for the nitrogen hyperfine coupling constant for the coordinated nitrogen of the imidazole ligand. These results have important implications for EPR and pulsed EPR studies of vanadoproteins.

Introduction

Vanadium is an important transition metal in biological systems because it is present in enzymes and it is able to mimic the effects of insulin.[1,2] The vanadyl ion, VO^{2+}, is a powerful structural probe in naturally occurring vanadoproteins and in systems where VO^{2+} is substituted for divalent cations, such as Mg^{2+} and Ca^{2+}, which are spectroscopically inaccessible.[3] Continuous wave (CW) electron paramagnetic resonance (EPR) and high-resolution EPR techniques, such as ESEEM (electron spin−echo envelope modulation) and ENDOR (electron nuclear double resonance), have been widely used to study the VO^{2+} ion in biological systems. The EPR spectra are typically interpreted by evaluating the EPR parameters, *g* and *A*, and then using empirical relationships to determine the coordinated ligands. In some cases, the EPR parameters are compared with the EPR parameters of model complexes with similar coordination spheres. Typically, vanadium ligand hyperfine coupling constants, (A_L), are too small to be resolved in the CW EPR spectrum. Experimentally, A_L values are often measured by high-resolution EPR techniques, such as ESEEM and ENDOR.

The CW EPR spectrum for the vanadyl ion, VO^{2+}(V^{4+}, d^1), depends on the local electronic and ligand environment of the vanadium center. The CW EPR spectrum for a rigid limit VO^{2+} system is dominated by the axial hyperfine interaction between the unpaired electron spin ($S = 1/2$) and the ^{51}V nuclear spin ($I = 7/2$, 99.8% natural abundance). The parallel components of the *g* and hyperfine (*A*) tensors are sensitive to the ligand environment and coordination of the vanadium center. The vanadium quadrupole coupling constant has also been shown to reflect the local electronic environment.[4,5]

Empirical additivity relationships are a useful tool for interpreting the EPR spectra of VO^{2+} complexes. The basis of the additivity relationship is that the vanadium hyperfine coupling constant, *A*, is sensitive to the number and type of equatorially coordinated ligands for an octahedral or square planar complex.[3] The additivity relationship for VO^{2+} complexes is given by the equation below:

$$A = \sum_i n_i A_i \qquad (1)$$

where n_i = the number of equatorial ligands of type *i* and A_i = the contribution to *A* from each equatorial ligand of type *i*. The additivity relationship can be used to calculate the vanadium hyperfine coupling constant, *A*, for a VO^{2+} complex if the number of equatorial ligands and the A_i values for each of the equatorial ligands are known.

In a recent study, Pecoraro and co-workers reported the use of the additivity relationship to predict the orientation of equatorial imidazole rings relative to the VO^{2+} bond in VO^{2+} model complexes.[6] Prior to Pecoraro's study, Cornman,[7] Chasteen,[3] and van Willigen[8] had each published different values for $A_{||}$(imidazole) that were used in the context of the additivity relationship to interpret the EPR spectra of VO^{2+} complexes with equatorial imidazole ligands. To address this issue, Pecoraro and co-workers synthesized five new VO^{2+} imidazole model complexes with the imidazole rings in different orientations with respect to the VO^{2+} bond.[6] They found that $A_{||}$ (imidazole contribution) varied from 120 to 138 MHz for parallel- and perpendicular-bound imidazole ligands, respectively. The additivity relationship and the newly found dependence of the vanadium *A* value on the imidazole ring orientation were used to interpret the EPR and ESEEM spectra of vanadium bromoperoxidase (VBrPO)[9] to estimate the orientation of the coordinated imidazole ligands.

Recent advances in computational chemistry have lead to the development of new methods for electronic structure calculations of *g* and *A* tensors for transition metals.[10−24] Several groups have reported computational methods for calculating *g* tensors.[14,17,22,23,25] The method of van Lenthe has been incorporated into a commercial software package, ADF (Amsterdam Density

* To whom correspondence should be addressed. Fax: 319-335-1270. E-mail: sarah-larsen@uiowa.edu.

10.1021/jp0215163 CCC: $22.00
Published on Web 09/26/2002

Functional Theory 2000.01),[26−29] which uses Slater type orbitals (STOs).[30] In the approach of van Lenthe, the spinor of the unpaired electron obtained from a density functional theory (DFT) calculation is used to calculate the *g* tensor for a Kramer's doublet open shell molecule. Spin−orbit (SO) coupling is included variationally using the zero-order regular approximation (ZORA) to the Dirac equation.[17] An analogous relativistic method for calculating *A* tensors was also developed by van Lenthe and was similarly incorporated into the ADF program.[18] Recently, the methods of van Lenthe have been applied to the calculation of EPR parameters for transition metal complexes.[16,19,31,32]

In this study, the effect of vanadyl−imidazole ring orientation on the EPR hyperfine and quadrupole coupling constants for a model complex will be investigated using DFT calculations of EPR parameters as implemented in the ADF program. A simple model complex, $[VO(imid)(H_2O)_4]^{2+}$, was constructed and geometry-optimized. The equatorially coordinated imidazole ring was then rotated relative to the V═O double bond, and DFT calculations of the EPR parameters were completed at each angle. The effects of imidazole ring orientation on the vanadium hyperfine and quadrupole interactions, as well as on the ligand hyperfine interaction of the coordinated nitrogen of the imidazole ring, were calculated. A comparison of the experimental and computational results will be discussed. The usefulness of DFT calculations of EPR parameters for interpreting the EPR spectra of vanadoproteins will also be assessed.

Theoretical Details

Geometry Optimization of $[VO(imid)(H_2O)_4]^{2+}$. To examine the effect of the imidazole ring orientation in VO^{2+} complexes, a model complex, $[VO(imid)(H_2O)_4]^{2+}$, was constructed with one imidazole ligand in the equatorial plane and with four water molecules as ligands (three in the equatorial plane and one axially coordinated). The geometry of this complex was optimized using the B3PW91[33,34] density functional the TZV[35] basis set with Gaussian 98.[36] A frequency calculation was performed to ensure that the geometry was at a minimum on the potential energy surface. The imidazole ring orientation was varied, and the calculations of EPR parameters described below were completed. The axes were chosen such that the V═O bond defined the *z*-axis and the V−N (imidazole) bond defined the *x*-axis.

Relativistic Calculations of EPR Parameters with ADF. The ADF program package (ADF 2000.01)[26−29] was used to calculate the EPR parameters for the VO^{2+} model complex. The methods for calculating *g* and *A* tensors developed by van Lenthe et al.[17−19] are implemented in ADF software. Relativistic effects are included using the ZORA Hamiltonian, which includes scalar relativistic (SR) and spin−orbit (SO) coupling. Two approaches can be used for *A* tensor calculations with ADF: the SR spin-unrestricted open shell Kohn Sham (SR UKS) calculation and the SO coupling and SR spin-restricted open shell Kohn Sham (SO + SR ROKS) calculation. In the SR UKS method, SO coupling is not included, but spin polarization effects are included making this the preferred method for calculating isotropic hyperfine coupling constants (A_{iso}).[19] In the SO + SR ROKS method, SO coupling effects are included but not spin polarization effects. The SO + SR ROKS method is used for calculating *g* tensors and the anisotropic contribution to the hyperfine coupling constants (A_D).

The BP86 density functional was used in the *g* and *A* tensor calculations. BP86 uses the parametrized electron gas data given by Vosko et al. for the LDA[37] with the correlation correction by Perdew.[33] The basis set V, which is a triple-ζ valence STO with two polarizable functions for atoms H through Ar, was used for all calculations and all atoms.[26−29]

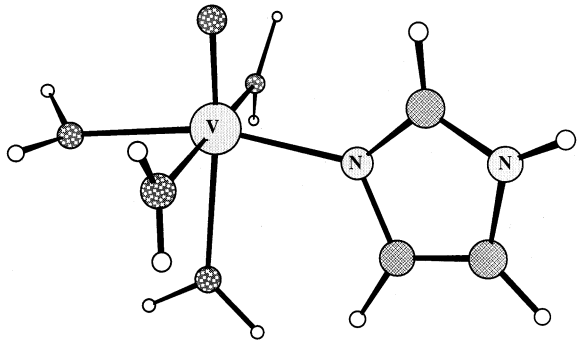

a) $[VO(imid)(H_2O)_4]^{2+}$

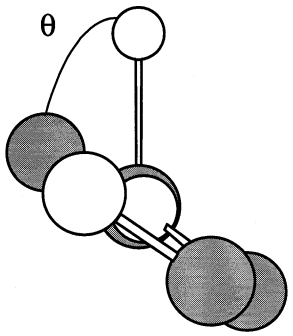

b)

Figure 1. (a) Structure of $[VO(imid)(H_2O)_4]^{2+}$ with $\theta = 0°$ and (b) the dihedral angle, θ, between V═O and the imidazole ring.

Results

DFT Calculations of the Vanadium Hyperfine Coupling Constants for the $[VO(imid)(H_2O)_4]^{2+}$ Model Complex. The optimized structure of $[VO(imid)(H_2O)_4]^{2+}$, with $\theta = 0$, is shown in Figure 1a. The dihedral angle, θ (Figure 1b), that characterizes the orientation of the imidazole ring relative to the V═O bond was varied from 0 to 345°. For each value of the dihedral angle, the vanadium hyperfine coupling constant, *A*, was calculated using the relativistic methods of van Lenthe.[17] The *A* values were calculated using two different methods, the SR UKS method (A_{iso}) and the SO + SR ROKS method (A_D). Spin polarization effects have not yet been incorporated into these SO-coupled equations for *A* value calculations. Therefore, the most accurate *A* values for transition metals when SO effects are nonnegligible are currently obtained by combining A_{iso} values calculated using the SR UKS method and A_D calculated using the SO + SR ROKS method.[19] The principal values of the *A* tensor, A_{11}, A_{22}, and A_{33}, are separated into an isotropic component (A_{iso}) and the dipolar components ($A_{D,x}$, $A_{D,y}$, $A_{D,z}$) according to the following equations:

$$\begin{aligned} A_{iso} &= (A_{11} + A_{22} + A_{33})/3 \\ A_{D,x} &= A_{11} - A_{iso} \\ A_{D,y} &= A_{22} - A_{iso} \\ A_{D,z} &= A_{33} - A_{iso} \end{aligned} \qquad (2)$$

The principal values of the *A* tensors for the $[VO(imid)(H_2O)_4]^{2+}$

TABLE 1: Calculated Vanadium Hyperfine Coupling Constant for $[VO(imid)(H_2O)_4]^{2+}$

	SR UKS[a,b]				SO + SR ROKS[a,b]				A_{iso} (SR UKS) + A_D (SO + SR ROKS)[a,b]		
angle (°)	A_{iso}	$A_{D,x}$	$A_{D,y}$	$A_{D,z}$	A_{iso}	$A_{D,x}$	$A_{D,y}$	$A_{D,z}$	A_{11}	A_{22}	A_{33} ($A_{\|\|}$)
0	−210	85	88	−173	−21	101	105	−206	−109	−106	−416
15	−211	85	87	−173	−20	102	104	−205	−109	−106	−416
30	−212	86	87	−173	−20	102	105	−206	−109	−107	−418
45	−214	86	88	−173	−20	103	106	−207	−110	−107	−421
60	−216	86	88	−174	−19	105	108	−209	−111	−108	−425
75	−218	86	88	−174	−19	105	109	−210	−112	−108	−428
90	−219	85	89	−174	−19	105	111	−211	−114	−108	−430
105	−219	85	90	−174	−19	104	112	−211	−115	−106	−429
120	−218	84	90	−174	−19	102	112	−209	−115	−105	−427
135	−216	83	90	−173	−19	101	112	−208	−115	−104	−423
150	−214	83	90	−173	−20	100	110	−207	−114	−103	−420
165	−212	83	89	−173	−20	99	108	−206	−113	−104	−418
180	−212	84	88	−173	−20	100	107	−206	−111	−105	−417
195	−212	85	88	−173	−20	101	105	−206	−110	−107	−418
210	−213	86	87	−173	−20	103	105	−207	−111	−108	−420
225	−215	85	88	−173	−20	103	107	−208	−112	−108	−422
240	−217	86	88	−174	−20	104	108	−209	−112	−109	−426
255	−218	86	88	−174	−19	106	109	−211	−113	−109	−429
270	−219	86	88	−175	−19	106	109	−211	−112	−110	−430
285	−218	86	88	−174	−19	106	109	−211	−112	−109	−430
300	−217	85	89	−174	−19	105	109	−210	−113	−108	−427
315	−215	85	89	−174	−20	103	108	−208	−112	−107	−424
330	−213	84	89	−173	−20	101	107	−207	−112	−106	−420
345	−211	85	88	−173	−20	101	106	−206	−110	−105	−417

[a] All A values in MHz. [b] BP86.

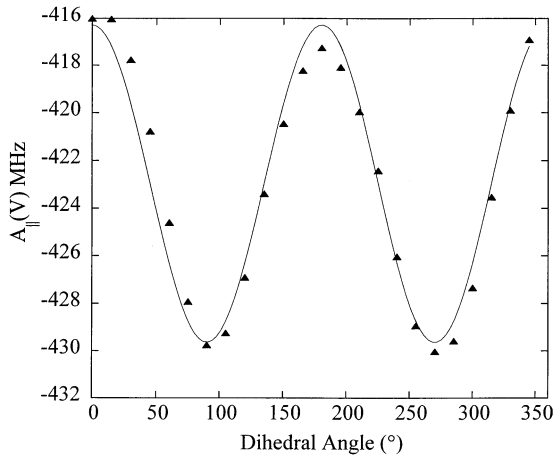

Figure 2. Calculated vanadium hyperfine coupling constant ($A_{||}$) for $[VO(imid)(H_2O)_4]^{2+}$ as a function of the dihedral angle, θ, is plotted using the data in Table 1. $A_{||}$ was calculated from A_{iso} (SR UKS, BP86) + A_D (SO + SR ROKS, BP86). The data were fit to $A_{||} = A + B(\sin 2\theta - 90)$ where $A = -423$ MHz and $B = -6.7$ MHz.

complexes calculated with the different methods and as a function of the dihedral angle are listed in Table 1. The combined A_{33} value (or $A_{||}$ value assuming axial symmetry) vs the dihedral angle is plotted in Figure 2. The calculated vanadium $A_{||}$ values vary systematically with dihedral angle.

Experimentally, Pecoraro and co-workers observed a similar functional dependence of the imidazole contribution to the hyperfine coupling constant on the orientation of the imidazole ring in VO^{2+}−imidazole model complexes.[6] The experimental data of Pecoraro and co-workers were fit to $A_{||}(\text{imid}) = A + B \sin(2\theta - 90)$ where A and B are fitted parameters and θ is the dihedral angle between V═O and the imidazole ring as pictured in Figure 1b. A least-squares fit of the calculated vanadium $A_{||}$ values for the $[VO(imid)(H_2O)_4]^{2+}$ model complex to the same functional form yields fitted parameters, $A = -423$ MHz and $B = -6.7$ MHz where $A_{||}(\text{vanadium}) = A + B \sin(2\theta - 90)$. The value of −423 MHz corresponds to the average $A_{||}$ value for $[VO(imid)(H_2O)_4]^{2+}$.

Use of the Additivity Relationship to Determine the Imidazole Contribution to the Vanadium Hyperfine Coupling Constant. To compare our computational results directly with the experimental data of Pecoraro and co-workers, the additivity relationship will be used to determine the parallel contribution of the equatorial imidazole ligand, $A_{||}(\text{imid})$, of $[VO(imid)(H_2O)_4]^{2+}$ to the overall parallel component of the vanadium hyperfine coupling constant. For each of the complexes synthesized by Pecoraro and co-workers, the contribution to $A_{||}$ due to the equatorial imidazole ligand was calculated by subtracting the contributions to $A_{||}$ from the other ligands using the additivity relationship. The experimental data demonstrate that the $A_{||}(\text{imid})$ contribution is dependent on the dihedral angle, θ, according to $A_{||}(\text{imid}) = A + B \sin(2\theta - 90)$ where A and B are fitted parameters equal to 128 and 9 MHz.[6]

The calculated EPR hyperfine coupling constants for $[VO(imid)(H_2O)_4]^{2+}$ can also be analyzed using the additivity relationship for comparison with the experimental data. For the $[VO(imid)(H_2O)_4]^{2+}$ complex, the imidazole contribution to $A_{||}$ is determined by subtracting the $A_{||}$ contribution due to the three equatorial water ligands from the calculated $A_{||}$ for the entire $[VO(imid)(H_2O)_4]^{2+}$ complex. The calculated value of 113.7 MHz from previous computational work[38] will be used as the $A_{||}$ contribution for an equatorial water molecule to the total parallel component of the hyperfine coupling constant. To obtain $A_{||}(\text{imid})$ for $[VO(imid)(H_2O)_4]^{2+}$, $3 \times (113.7) = 341$ MHz was subtracted from the calculated $|A_{33}|$ (combined SR UKS (A_{iso}) and SO + SR ROKS (A_D), BP86). The results for the calculated $|A_{||}|$ imidazole contribution as a function of dihedral angle are listed in Table 2. The computational results (combined SR UKS (A_{iso}) and SO + SR ROKS (A_D), BP86) were scaled by an additive constant equal to 46 MHz to facilitate a comparison with the experimental data. The computational results are plotted in Figure 3. For comparison, the solid curve was calculated from the fit to the experimental data of Pecoraro and co-workers.[6] The computational data reproduce the functional dependence

TABLE 2: Calculated $A_{||}$ (Imidazole Contribution) and Principal Values of the Vanadium Quadrupole Coupling Constant Calculated with SR UKS (BP86)

angle (°)	$\|A_{||}$(imidazole)$\|^{a,b,c}$	$P_{xx}{}^a$	$P_{yy}{}^a$	$P_{zz}{}^a$
0	75	0.08	0.01	−0.09
15	75	0.08	0.01	−0.09
30	77	0.08	0.02	−0.10
45	80	0.08	0.03	−0.11
60	83	0.08	0.03	−0.11
75	87	0.08	0.04	−0.12
90	89	0.09	0.04	−0.12
105	88	0.09	0.04	−0.12
120	86	0.09	0.03	−0.12
135	82	0.08	0.03	−0.11
150	79	0.08	0.02	−0.10
165	77	0.08	0.01	−0.10
180	76	0.08	0.01	−0.09
195	77	0.08	0.01	−0.09
210	79	0.08	0.02	−0.10
225	81	0.08	0.02	−0.11
240	85	0.09	0.03	−0.11
255	88	0.09	0.03	−0.12
270	89	0.09	0.04	−0.12
285	88	0.09	0.04	−0.12
300	86	0.08	0.03	−0.12
315	82	0.08	0.03	−0.11
330	79	0.08	0.02	−0.10
345	76	0.08	0.02	−0.10

[a] $A_{||}$ and P values in MHz. [b] A_{iso} (SR UKS) + A_D (SR + SO ROKS) BP86. [c] To obtain $|A_{||}$(imidazole)|, 341 MHz (3 × 113.7($A_{||}$(H_2O))) has been subtracted from the vanadium $A_{||}$.

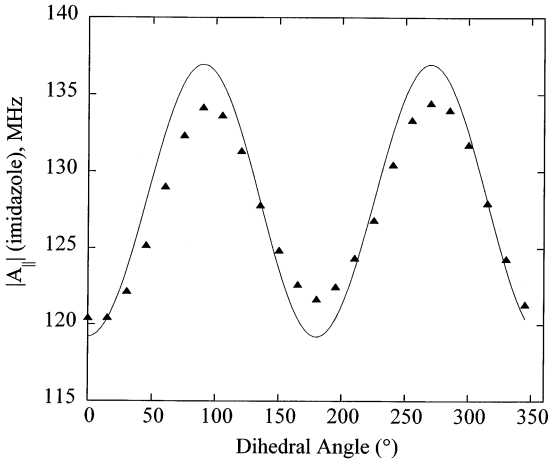

Figure 3. Comparison of the orientation dependence of the calculated $|A_{||}|$ (imidazole contribution) for $[VO(imid)(H_2O)_4]^{2+}$ and the experimental results of Pecoraro and co-workers is presented. The calculated $|A_{||}|$ (imidazole contribution) was obtained using the calculated $|A_{||}|$ values (A_{iso} (SR UKS, BP86) + A_D (SO + SR ROKS, BP86)) from which the 341 MHz contribution from the three equatorial water molecules was subtracted. The filled triangles represent the calculated $|A_{||}|$(imidazole) values from Table 2 that have been shifted by 46 MHz in order to facilitate a comparison with the experimental data. The solid line represents the fit, $A + B\sin(2\theta - 90)$ where $A = 128$ and $B = 9$ MHz to the experimental data of Pecoraro and co-workers.

of $A_{||}$(imidazole) on the dihedral angle quite well, after applying an additive scaling factor to the calculated values.

DFT Calculations of the Nitrogen Hyperfine Coupling Constants for a $[VO(imid)(H_2O)_4]^{2+}$ Model Complex. The nitrogen hyperfine coupling constants for the coordinated nitrogen (N3) of the imidazole ligand of the $[VO(imid)(H_2O)_4]^{2+}$ were also calculated and are listed in Table 3. The nitrogen hyperfine coupling constant can be decomposed into three contributions, $A_{iso} = A_0^0$, A_2^0 (the axial hyperfine coupling constant), and A_2^2 (the rhombic component of the hyperfine coupling constant), as defined by the equations below:[39]

$$A_0^0 = \mathrm{Tr}A/3$$

$$A_2^0 = (A_{33} - A_0^0)/2$$

$$A_2^2 = (A_{22} - A_{11})/2$$

$$\text{where } |A_{11}| < |A_{22}| < |A_{33}| \qquad (3)$$

where A is the hyperfine coupling constant matrix and A_{11}, A_{22}, and A_{33} are the principal values of A. To assess the importance of the SO contribution to the nitrogen hyperfine coupling constant for the coordinated nitrogen (N3), a calculation of the hyperfine tensor for $[VO(imid)(H_2O)_4]^{2+}$ with a dihedral angle of 0 with the SR ROKS method was completed. The results of this calculation were $A_{iso} = 0$ and $A_{D,x} = 0.65$, $A_{D,y} = 0.48$, and $A_{D,z} = -1.13$ MHz. When compared with the results of the SO + SR ROKS calculation in Table 3, these results show that SO contributions to the dipolar component of the hyperfine tensor are on the order of 10−20%. Therefore, the three components of the hyperfine coupling constant $A_{iso} = A_0^0$, A_2^0, and A_2^2 were obtained by combining the calculated values, such that A_{iso} is taken from the SR UKS calculation and the anisotropic contributions are taken from the SO + SR ROKS calculation. The results are listed in the last column of Table 3. A graph of the variation of A_{iso}(N3), A_2^0, and A_2^2 as a function of the dihedral angle, θ, is shown in Figure 4. A_{iso}(N3) exhibits the same functional dependence as $A_{33}(^{51}V)$. The data in Figure 4 can be fit to the same functional form as $A_{||}(^{51}V)$, where $A_{iso}(N3) = A_{N3} + B_{N3}\sin(2\theta - 90)$ with $A_{N3} = -7.47$ MHz and $B_{N3} = -0.59$ MHz. A_{N3} is equal to the isotropic coupling constant averaged over all of the angles. The angular dependence of A_2^0 and A_2^2 is relatively small in magnitude as compared to A_{iso} as illustrated by Figure 4.

Experimentally, nitrogen hyperfine coupling constants for vanadyl complexes are measured by ESEEM and ENDOR spectroscopy.[8,40−44] Experimental data are not available for a quantitative comparison of the computational results for the nitrogen hyperfine coupling constants. The calculated value of A_{iso} for $[VO(imid)(H_2O)_4]^{2+}$ ranges from −8.1 to −6.8 MHz depending on the dihedral angle. These values are ∼10−20% higher than similar experimental A_{iso} values for the coordinated nitrogen of vanadyl−imine complexes that range from approximately 6−7 MHz.[41]

DFT Calculations of the Vanadium Quadrupole Coupling Constant. Recently, pulsed ENDOR spectroscopy has been used to measure the ^{51}V quadrupole coupling constant.[4,5] The vanadium quadrupole coupling constant was shown to be particularly sensitive to axial coordination relative to the V=O bond and to equatorial ligand geometry. The equations for the quadrupole parameters, $P_{||}$ and η, are given below:

$$P_{||} = \frac{3}{2}P_{zz} = \frac{3e^2qQ}{4I(2I-1)} = \frac{3e^2qQ}{84}\left(\text{for } I = \frac{7}{2}\right)$$

$$\eta = \left|\frac{P_{xx} - P_{yy}}{P_{zz}}\right| \qquad (4)$$

where P_{xx}, P_{yy}, and P_{zz} are the principal values of the traceless quadrupole tensor, P, q is the field gradient along the principal axis of the largest field gradient (z-axis), and Q is the nuclear quadrupole moment (-0.05×10^{-24} cm^2).[4]

TABLE 3: Calculated Nitrogen Hyperfine Coupling Constant of the Coordinated Nitrogen (N3) of $[VO(imid)(H_2O)_4]^{2+}$

	SR UKS[a,b]				SO + SR ROKS[a,b]				A_{iso} (SR UKS) + A_D (SO + SR ROKS)[a,b]	
angle (°)	A_{iso}	$A_{D,x}$	$A_{D,y}$	$A_{D,z}$	A_{iso}	$A_{D,x}$	$A_{D,y}$	$A_{D,z}$	A_2^0	A_2^2
0	−6.91	0.20	0.05	−0.25	0.06	0.58	0.39	−0.98	−0.49	−0.10
15	−6.96	0.21	0.07	−0.27	0.06	0.60	0.38	−0.97	−0.49	−0.11
30	−7.16	0.22	0.12	−0.34	0.05	0.67	0.25	−0.92	−0.46	−0.21
45	−7.44	0.25	0.18	−0.43	0.04	0.80	0.04	−0.85	−0.42	−0.38
60	−7.75	0.27	0.22	−0.49	0.04	0.94	−0.16	−0.78	−0.39	−0.55
75	−7.98	0.29	0.22	−0.51	0.03	1.04	−0.29	−0.75	−0.38	−0.67
90	−8.09	0.30	0.20	−0.50	0.03	1.10	−0.35	−0.75	−0.38	−0.72
105	−8.04	0.30	0.19	−0.49	0.04	1.09	−0.33	−0.76	−0.38	−0.71
120	−7.88	0.28	0.20	−0.48	0.06	1.04	−0.27	−0.77	−0.38	−0.65
135	−7.55	0.25	0.21	−0.45	0.09	0.94	−0.15	−0.80	−0.40	−0.54
150	−7.27	0.22	0.16	−0.38	0.10	0.82	0.03	−0.85	−0.42	−0.40
165	−6.97	0.21	0.08	−0.28	0.09	0.70	0.22	−0.92	−0.46	−0.24
180	−6.80	0.19	0.02	−0.21	0.12	0.64	0.31	−0.95	−0.48	−0.16
195	−6.82	0.19	0.01	−0.20	0.11	0.63	0.31	−0.94	−0.47	−0.16
210	−7.04	0.21	0.07	−0.27	0.10	0.69	0.21	−0.90	−0.45	−0.24
225	−7.31	0.24	0.12	−0.36	0.08	0.80	0.04	−0.84	−0.42	−0.38
240	−7.63	0.28	0.14	−0.43	0.06	0.93	−0.15	−0.78	−0.39	−0.54
255	−7.89	0.31	0.14	−0.45	0.06	0.93	−0.15	−0.78	−0.39	−0.54
270	−8.00	0.32	0.13	−0.45	0.05	1.07	−0.33	−0.74	−0.37	−0.70
285	−8.00	0.33	0.13	−0.46	0.05	1.07	−0.33	−0.75	−0.37	−0.70
300	−7.85	0.33	0.13	−0.46	0.04	1.01	−0.25	−0.75	−0.38	−0.63
315	−7.61	0.30	0.12	−0.42	0.04	0.88	−0.09	−0.79	−0.40	−0.48
330	−7.32	0.25	0.09	−0.35	0.05	0.74	0.13	−0.87	−0.43	−0.30
345	−7.05	0.22	0.06	−0.28	0.05	0.62	0.32	−0.94	−0.47	−0.15

[a] All A values in MHz. [b] BP86.

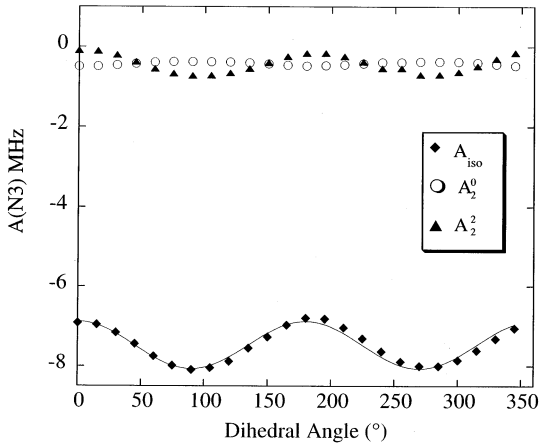

Figure 4. Graph of the calculated isotropic hyperfine coupling constant of the coordinated nitrogen (N3) for $[VO(imid)(H_2O)_4]^{2+}$ as a function of the dihedral angle, θ, is plotted using the data in Table 3 (SR UKS, BP86). The data were fit to A_{iso} (N3) = $A + B \sin(2\theta - 90)$ where $A = -7.47$ MHz and $B = -0.59$ MHz. The anisotropic parts of the nitrogen hyperfine coupling constant, A_2^0 and A_2^2 obtained by combining A_{iso} (SR UKS) and A_D (SO + SR ROKS) are also plotted.

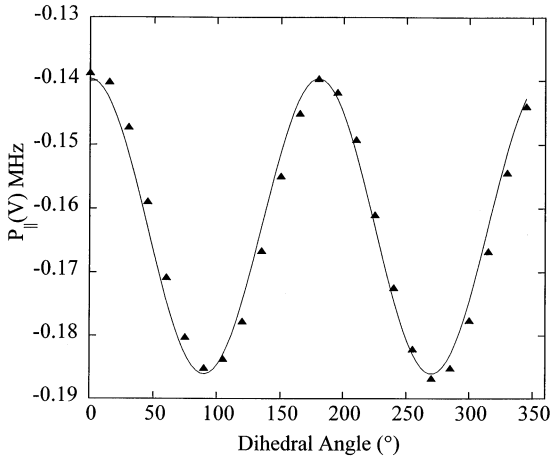

Figure 5. Graph of the calculated vanadium quadrupole coupling constant ($P_{||}$) for $[VO(imid)(H_2O)_4]^{2+}$ as a function of the dihedral angle, θ, is plotted using the data in Table 2 (SR UKS, BP86). The data were fit to $P_{||}(V) = P + B \sin(2\theta - 90)$ where $P = -0.16$ MHz and $B = -0.023$ MHz.

In the study reported here, $P_{||}$ of vanadium was calculated using the SR UKS relativistic method with the BP86 functional. The results are listed in Table 2 and are plotted in Figure 5. The orientation dependence of the nuclear quadrupole parameter, $P_{||}$, follows the same orientation dependence as the vanadium and nitrogen hyperfine coupling constants.

Discussion

Dependence of Vanadium Hyperfine Coupling Constants on Equatorial Imidazole Ring Orientation. The additivity relationship has been used extensively and successfully to interpret the EPR spectra of VO^{2+} complexes. The basis for the additivity relationship is that each equatorial ligand contributes a characteristic vanadium hyperfine coupling value that is independent of the other ligands present in the complex. These characteristic vanadium hyperfine coupling values for each ligand in the complex are then summed to calculate the total vanadium hyperfine coupling constant for the complex. The additivity relationship fails to predict vanadium hyperfine coupling constants when the additive hyperfine coupling is dependent on some other structural parameter, such as orientation. However, if this orientation dependence can be predicted using electronic structure calculations, then valuable structural information can potentially be obtained from the EPR spectrum.

The DFT calculations of the vanadium hyperfine coupling constants for $[VO(imid)(H_2O)_4]^{2+}$ as a function of imidazole ring orientation clearly show that the vanadium hyperfine coupling constant sensitively depends on the imidazole ring orientation as shown in Figure 2. This angular dependence of the vanadium hyperfine coupling constant was first observed by Pecoraro and co-workers.[6] In their study, vanadyl−imidazole complexes were synthesized with the imidazole ring in different

orientations relative to the VO bond. By analyzing the EPR spectra of these model complexes using the additivity relationship, Pecoraro and co-workers demonstrated that the imidazole contribution to the vanadium hyperfine coupling constant depended on the dihedral angle between the imidazole ring and the V═O bond according to $A_{||}(\text{imid}) = A + B\sin(2\theta - 90)$ where $A = 128$ MHz and $B = 9$ MHz. Pecoraro and co-workers attributed this functional dependence to the fact that the overlap integral between the vanadium d_{xy} orbital and the nitrogen aromatic p orbital that depends on the dihedral angle, θ, is $\int \sin^2\theta\, d\theta$. This can be evaluated to give $-\cos 2\theta$ or $\sin(2\theta - 90)$, which is the observed functional dependence of $A_{||}$(imid).[6]

The DFT calculations of the vanadium hyperfine coupling constants for the $[VO(imid)(H_2O)_4]^{2+}$ model complex clearly reproduce the experimental trend in the vanadium hyperfine coupling constants observed by Pecoraro. The total variation of the parallel component of the vanadium hyperfine coupling constant with imidazole ring orientation spans ∼14 MHz. However, while the DFT calculations of the vanadium hyperfine coupling constants are qualitatively correct, the quantitative agreement is still insufficient for a direct comparison with experimental data. Because the calculated values are systematically too low, the agreement between experiment and theory can be improved by empirically scaling the calculated values. The calculated hyperfine coupling constants (imidazole contribution) graphed in Figure 3 have been scaled by an additive constant of 46 MHz to facilitate a comparison with the experimental data.

The variation of the imidazole contribution to the parallel component of the vanadium hyperfine coupling constant that is plotted in Figure 3 provides a direct comparison of the experimental data generated by Pecoraro and co-workers and the DFT data from our vanadyl−imidazole model complex. The agreement between the fit to the experimental data and the scaled calculated values for $A_{||}$(imidazole) is very good. However, the utility of these computational methods for interpreting experimental EPR data is undermined by the poor quantitative agreement with experimental model complex data.

To better understand the deviation of the calculated and the experimental vanadium hyperfine coupling constants, the isotropic (A_{iso}) and dipolar (A_D) components of the vanadium hyperfine coupling constant should be considered separately. Accurate calculation of the isotropic hyperfine coupling constant for a transition metal, such as vanadium, depends on the inclusion of spin polarization since this is the primary mechanism responsible for the isotropic hyperfine coupling between the unpaired electron and the transition metal nucleus. Kaupp and co-workers have shown that generalized gradient correction (GGA) functionals substantially underestimate spin polarization but that hybrid functionals, such as BHP86, are able to reproduce spin polarization effects much more accurately.[10,12] Unfortunately, hybrid functionals are not available in ADF software and consequently, the ADF calculations underestimate spin polarization contributions to A_{iso}. SO contributions to the isotropic hyperfine coupling constant may also be significant but are not currently included in ADF calculations that also include spin polarization. The dipolar hyperfine coupling constant is much less sensitive to the inclusion of spin polarization effects; therefore, SO calculations that do not include spin polarization are sufficient for accurate calculations. Future improvements in the ADF methods such as the inclusion of SO coupling and spin polarization in the same calculation may significantly improve the quantitative agreement of these calculations with experimental data.[17]

Dependence of Equatorial Imidazole Nitrogen Hyperfine Coupling Constants on Imidazole Ring Orientation. The results of the DFT calculations reported here indicate that the nitrogen hyperfine coupling constant for the coordinated nitrogen (N3) of the imidazole ring in $[VO(imid)(H_2O)_4]^{2+}$ also depends on the orientation of the imidazole ring relative to the V═O bond. The isotropic hyperfine coupling constant for the coordinated nitrogen varies from approximately −6.8 to −8.1 MHz at dihedral angles of 180 and 90°, respectively, as shown in Figure 4. This is a variation of the isotropic hyperfine coupling constant of approximately 10% depending on the orientation of the imidazole ring in the vanadyl complex. The variation of the nitrogen isotropic hyperfine coupling constant follows the functional form of $\sin(2\theta - 90)$ described by Pecoraro and co-workers for the imidazole contribution to the vanadium hyperfine coupling constant.[6] ESEEM experiments are frequently used to directly measure nitrogen hyperfine coupling constants for ligands coordinated to VO^{2+}. Literature data for the isotropic nitrogen hyperfine coupling constants of vanadyl model complexes indicate values of 6−7 MHz for imine nitrogens in vanadyl complexes.[41] The calculated isotropic nitrogen hyperfine coupling constant (A_{iso}) for the coordinated nitrogen of imidazole ranges from about −6.8 to −8.1 MHz. The calculated values are systematically higher than experimental values by approximately 15%. However, this is just an estimate since a direct comparison between theory and experiment is not available for this complex. A more complete computational study of nitrogen ligand hyperfine in VO^{2+} complexes is in progress.

Because nitrogen hyperfine coupling constants can be measured directly using ESEEM or ENDOR, the nitrogen hyperfine coupling constant could potentially give a direct measurement of the imidazole ring orientation. For example, if equatorial ligation of two imidazole rings to V═O occurs, the DFT results could be used to determine the relative orientations of the two rings based on the relative values of the N3 hyperfine coupling constants. Van Willigen and co-workers measured the nitrogen ENDOR spectrum for $VO(Im)_4^{2+}$ and found two different nitrogen coupling constants, $A_z = 6.6$ and 7.4 MHz.[8] They assigned the two nitrogen hyperfine coupling constants to the coordinated and remote nitrogen, respectively, of the imidazole ring. An alternate interpretation supported by the computational results reported here would be that the signals are both due to the coordinated imidazole rings in which the imidazole rings have two different orientations with respect to the V═O bond, one being approximately parallel and the other being approximately perpendicular.

Theoretical Basis for the Orientation Dependence of the Vanadium and Nitrogen Hyperfine Coupling Constants. The unpaired electron in a typical vanadyl (VO^{2+}) complex with C_{4v} symmetry is primarily located in the nonbonding vanadium d_{xy} orbital.[3,45] Pecoraro and co-workers proposed that the basis for the orientation dependence of the hyperfine coupling constants for the imidazole ligand is the overlap between the aromatic p orbital on the coordinated nitrogen (N3) and the vanadium d_{xy} orbital.[6] As the imidazole ring is rotated from a parallel ($\theta = 0°$) to perpendicular ($\theta = 90°$) orientation relative to the V═O bond, the overlap between the aromatic p orbital on the imidazole N3 and the vanadium d_{xy} orbital decreases. This results in an increase in the metal character of the singly occupied molecular orbital (SOMO) and a concomitant increase in $A_{||}$. This trend is reflected in the DFT calculations reported here. The calculated percentages of vanadium d_{xy} orbital and nitrogen (N3) aromatic p_y orbital contributions to the SOMO vs the dihedral angle, θ, are plotted in Figure 6. (Percentages

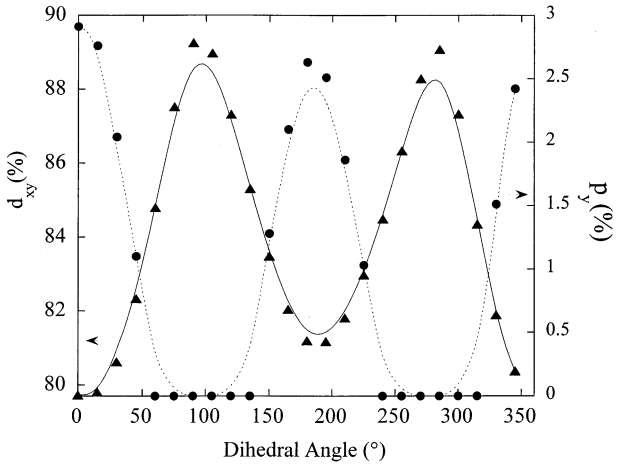

Figure 6. Calculated percentage contributions (SR UKS) of vanadium d_{xy} (filled triangles) and nitrogen p_y (filled circles) orbitals to the SOMO of the $[VO(imid)(H_2O)_4]^{2+}$ complex as a function of the dihedral angle. Contributions less than 1% are not listed in the output code and appear as 0% on the graph. The solid line is just a smooth fit to the data.

less than 1% are not listed in the ADF output; therefore, all percentages less than 1% are plotted as 0% in the graph. This accounts for the flat portion of the p_y graph.) As the N3 p_y orbital contribution decreases going from $\theta = 0°$ to $\theta = 90°$, the vanadium d_{xy} percentage increases. This trend follows the observed variation in $A_{||}$ as well and supports Pecoraro's explantion.

Dependence of the Vanadium Quadrupole Coupling Constant on the Imidazole Ring Orientation. Britt and co-workers recently reported pulsed ENDOR measurements of the vanadium quadrupole coupling constants for vanadyl complexes and corresponding DFT calculations of the vanadium nuclear quadrupole coupling constants using Gaussian software.[4,5] For $VO(H_2O)_5^{2+}$, $P_{||}$, the calculated nuclear quadrupole parameter, was -0.185 MHz as compared to an experimental value of -0.20 MHz.[4,5] Axial ligation and geometry distortions in the equatorial plane effect the size of vanadium $P_{||}$. For the $[VO(imid)(H_2O)_4]^{2+}$ complex studied here, $P_{||}$ varied from -0.14 to -0.19 MHz depending on the dihedral angle. The orientation dependence of the calculated vanadium $P_{||}$ with dihedral angle mirrored the orientation dependence of the hyperfine coupling constants. The DFT calculations may be used in the future to guide the interpretation of experimental vanadium nuclear quadrupole data.

Using DFT Calculations to Interpret the EPR Spectra of VO^{2+} in Biological Systems. EPR spectroscopy has been used to investigate VO^{2+} in biological systems such as VO^{2+}-apoferritin, VO^{2+}-transferrin, reduced vanadium bromoperoxidase (VBrPO), VO^{2+}-substituted imidazole glycerol phosphate dehydratase, and VO^{2+}-substituted D-xylose isomerase.[40−44,46−49] For example, the CW EPR spectrum of reduced VBrPO can be analyzed using the additivity relationship and the following ligand set ($\perp$ imidazole, || imidazole, and alkoxide, hydroxide (low pH), or water (high pH)). As discussed in detail by Pecoraro and co-workers, the agreement between the experimental data and the A values calculated using the additivity relationship with different A values for perpendicular and parallel coordinated imidazole, respectively, is very good.[6] The computational results reported here suggest that calculations of the EPR parameters for proposed active site structures could potentially be used to support or exclude proposed structures based on a comparison of the experimental data and the calculated values. This procedure is still limited by the lack of quantitative agreement between the calculated and the experimental values. However, the results reported here show that trends in EPR parameters such as hyperfine coupling constants can be qualitatively reproduced by the DFT calculations.

In our study, we have shown that the nitrogen hyperfine coupling constants for equatorially coordinated imidazole ligands also depend on the orientation of the imidazole ring relative to the V═O bond. Experimentally, nitrogen hyperfine coupling constants in VO^{2+} complexes are measured by ESEEM or ENDOR experiments. The advantage of ESEEM or ENDOR experiments is that the vanadium nitrogen hyperfine coupling constants of the coordinated nitrogen (N3) are directly probed. By comparison, in CW EPR experiments, the effect of all of the ligands on the vanadium hyperfine interaction must be factored in using the additivity relationship.

A survey of previous VO^{2+} model complex and protein ESEEM and ENDOR studies has shown that nitrogen hyperfine coupling constants for equatorially coordinated imidazole ligands generally fall in the range of 6−7 MHz. This range of nitrogen hyperfine coupling constants may reflect differences in the orientation of the equatorial imidazole ring. Unfortunately, adequate experimental data are not available for comparison with the calculated nitrogen hyperfine data. ESEEM experiments on Pecoraro's model complexes would provide a starting point for these comparisons. DFT calculations can be particularly helpful for cases in which model complexes are not available. For example, axial imidazole ligation to VO^{2+} has been proposed in other systems,[9] but good predictions of the expected hyperfine coupling constants do not exist. With further improvements in the quantitative agreement of calculated with experimental EPR parameters, DFT calculations may be used to calculate EPR parameters for proposed active site structures in vanadyl complexes.

Conclusions

DFT calculations of the EPR parameters for a model vanadyl−imidazole complex, $[VO(imid)(H_2O)_4]^{2+}$, were used to investigate the orientation dependence of the hyperfine coupling constants (vanadium and nitrogen). The DFT calculations illustrated that the vanadium hyperfine coupling constant varies according to $A_{||} = A + B \sin(2\theta - 90)$ (where θ is the dihedral angle between V═O and the imidazole ring) as predicted by Pecoraro and co-workers.[6] In addition, the orientation dependence of the hyperfine coupling constant for the coordinated nitrogen of the imidazole ring was found to follow the same functional form but with different values for *A* and *B*. The calculated values for the hyperfine coupling constants deviated systematically from the experimental data, but the trends in the coupling constants agreed very well with the experimental results. The orientation dependence was discussed in the context of the changes in the calculated percentage composition of the SOMO for the vanadyl−imidazole complex. It was found that as the nitrogen p aromatic orbital contribution decreased and the d_{xy} orbital contribution increased, $A_{||}$ increased. Vanadium nuclear quadrupole coupling constants were also calculated for the model complex. Application of these computational results to biological systems was discussed.

Acknowledgment. S.L. gratefully acknowledges the support of NSF (CHE-02048047) and the University of Iowa (Carver). Erik van Lenthe is acknowledged for assistance with SR ROKS calculations. The calculations were performed on an SGI octane workstation obtained through an NSF grant (CTS-99-73431) and on the supercomputer through the National Computational Science Alliance (CHE010042).

Supporting Information Available: Optimized Cartesian coordinates for $[VO(imid)(H_2O)_4]^{2+}$. This material is available free of charge via the Internet at http://pubs.acs.org.

References and Notes

(1) Baran, E. J. *J. Inorg. Biochem.* **2000**, *80*, 1−10.

(2) Thompson, K. H.; McNeill, J. H.; Orvig, C. *Chem. Rev.* **1999**, *99*, 2561−2571.

(3) Chasteen, N. D. Vanadyl(IV) EPR Spin Probes: Inorganic and Biochemical Aspects. In *Biological Magnetic Resonance*; Berliner, L. J., Reuben, J., Eds.; Plenum: New York, 1981; Vol. 3, p 53.

(4) Grant, C. V.; Geiser-Bush, K. M.; Cornman, C. R.; Britt, R. D. *Inorg. Chem.* **1999**, *38*, 6285−6288.

(5) Grant, C. V.; Cope, W.; Ball, J. A.; Maresch, G. G.; Gaffney, B. J.; Fink, W.; Britt, R. D. *J. Phys. Chem. B* **1999**, *103*, 10627−10631.

(6) Smith, T. S., II; Root, C. A.; Kampf, J. W.; Rasmussen, P. G.; Pecoraro, V. L. *J. Am. Chem. Soc.* **2000**, *122*, 767−775.

(7) Cornman, C. R.; Geiser-Bush, K. M.; Rowley, S. P.; Boyle, P. D. *Inorg. Chem.* **1997**, *36*, 6401−6408.

(8) Mulks, C. F.; Kirste, B.; van Willigen, H. *J. Am. Chem. Soc.* **1982**, *104*, 5906−5911.

(9) LoBrutto, R.; Hamstra, B. J.; Colpas, G. J.; Pecoraro, V. L.; Frasch, W. D. *J. Am. Chem. Soc.* **1998**, *120*, 4410−4416.

(10) Munzarova, M. L.; Kaupp, M. *J. Phys. Chem. B.* **2001**, *105*, 12644−12652.

(11) Munzarova, M. L.; Kubacek, P.; Kaupp, M. *J. Am. Chem. Soc.* **2000**, *122*, 11900−11913.

(12) Munzarova, M.; Kaupp, M. *J. Phys. Chem. A* **1999**, *103*, 9966−9983.

(13) Kaupp, M.; Reviakine, R.; Malkina, O. L.; Arbuznikov, A.; Schimmelpfennig, B.; Malkin, V. G. *J. Comput. Chem.* **2002**, *23*, 794.

(14) Malkina, O. L.; Vaara, J.; Schimmelpfennig, B.; Munzarova, M.; Malkin, V. G.; Kaupp, M. *J. Am. Chem. Soc.* **2000**, *122*, 9206−9218.

(15) Neese, F. *J. Chem. Phys.* **2001**, *115*, 11080.

(16) van Lenthe, E.; van der Avoird, A.; Hagen, W. R.; Reijerse, E. J. *J. Phys. Chem. A* **2000**, *104*, 2070−2077.

(17) van Lenthe, E.; Wormer, P. E. S.; van der Avoird, A. *J. Chem. Phys.* **1997**, *107*, 2488−2498.

(18) van Lenthe, E.; van der Avoird, A.; Wormer, P. E. S. *J. Chem. Phys.* **1998**, *108*, 4783−4796.

(19) Stein, M.; van Lenthe, E.; Baerends, E. J.; Lubitz, W. *J. Phys. Chem. A* **2001**, *105*, 416−425.

(20) Neese, F. *J. Phys. Chem. A* **2001**, *105*, 4290−4299.

(21) Neese, F. *Int. J. Quant. Chem.* **2001**, *83*, 104−114.

(22) Patchkovskii, S.; Ziegler, T. *J. Am. Chem. Soc.* **2000**, *122*, 3506−3516.

(23) Patchkovskii, S.; Ziegler, T. *J. Chem. Phys.* **1999**, *111*, 5730−5740.

(24) Patchkovskii, S.; Ziegler, T. *J. Phys. Chem. A* **2001**, *105*, 5490−5497.

(25) Schreckenbach, G.; Ziegler, T. *J. Phys. Chem. A* **1997**, *101*, 3388−3399.

(26) Baerends, E. J.; Ellis, D. E.; Ros, P. *Chem. Phys*. **1973**, *2*, 41−51.

(27) Versluis, L.; Ziegler, T. *J. Chem. Phys.* **1988**, *88*, 322−328.

(28) Te Velde, G.; Baerends, E. J. *J. Comput. Phys.* **1992**, *99*, 84−98.

(29) Guerra, C. F.; Snijders, J. G.; Te Velde, G.; Baerends, E. J. *Theor. Chem. Acc.* **1998**, *99*, 391−403.

(30) Slater, J. C. *Phys. Rev.* **1930**, *36*, 57.

(31) Larsen, S. C. *J. Phys. Chem. A* **2001**, *105*, 8333−83338.

(32) Carl, P. J.; Isley, S. L.; Larsen, S. C. *J. Phys. Chem. A* **2001**, *108*, 4563−4573.

(33) Perdew, J. P. *Phys. Rev. B* **1986**, *33*, 8822−8824.

(34) Becke, A. D. *J. Chem. Phys.* **1993**, *98*, 5648−5652.

(35) Schafer, A.; Huber, C.; Ahlrichs, R. *J. Chem. Phys.* **1994**, *100*, 5829−5835.

(36) Frisch, M. J.; Trucks, G. W.; Schlegel, H. B.; Scuseria, G. E.; Robb, M. A.; Cheeseman, J. R.; Zakrzewski, V. G.; Montgomery, J. J. A.; Stratmann, R. E.; Burant, J. C.; Dapprich, S.; Millam, J. M.; Daniels, A. D.; Kudin, K. N.; Strain, M. C.; Farkas, O.; Tomasi, J.; Barone, V.; Cossi, M.; Cammi, R.; Mennucci, B.; Pomelli, C.; Adamo, C.; Clifford, S.; Ochterski, J.; Petersson, G. A.; Ayala, P. Y.; Cui, Q.; Morokuma, K.; Malick, D. K.; Rabuck, A. D.; Raghavachari, K.; Foresman, J. B.; Cioslowski, J.; Ortiz, J. V.; Baboul, A. G.; Stefanov, B. B.; Liu, G.; Liashenko, A.; Piskorz, P.; Komaromi, I.; Gomperts, R.; Martin, R. L.; Fox, D. J.; Keith, T.; Al-Laham, M. A.; Peng, C. Y.; Nanayakkara, A.; Gonzalez, C.; Challacombe, M.; Gill, P. M. W.; Johnson, B. G.; Chen, W.; Wong, M. W.; Andres, J. L.; Head-Gordon, M.; S. R. E.; Pople, J. A. *Gaussian 98*, Revision A.6; Gaussian, Inc.: Pittsburgh, PA, 1998.

(37) Vosko, S. H.; Wilk, L.; Nusair, M. *Can. J. Phys.* **1980**, *58*, 1200.

(38) Saladino, A. C.; Larsen, S. C. $A_{33} = 455$ MHz for $VO(H_2O)_5^{2+}$ obtained from ADF calculations (BP86, A_{iso} (SRUKS) + A_D (SO + SR ROKS), unpublished results.

(39) Gerfen, G. J.; Bellew, B. F.; Singel, D. J. *Chem. Phys. Lett.* **1991**, *180*, 490−496.

(40) Eaton, S. S.; Dubach, J.; More, K., M.; Eaton, G. R.; Thurman, G.; Ambruso, D. R. *J. Biol. Chem.* **1989**, *264*, 4776−4781.

(41) Fukui, K.; Ohya-Nishiguchi, H.; Kamada, H. *Inorg. Chem.* **1998**, *37*, 2326−2327.

(42) Dikanov, S. A.; Tyryshkin, A. M.; Huttermann, J.; Bogumil, R.; Witzel, H. *J. Am. Chem. Soc.* **1995**, *117*, 4976−4986.

(43) *ESEEM of Nitrogen Coordinated Oxo-Vanadium(IV) Complexes*; Riejerse, E. J., Shane, J., de Boer, E., Collison, D., Eds.; World Scientific Publishers: Singapore City, 1989.

(44) de Boer, E.; Keijzers, C. P.; Reijerse, E. J.; Collison, D.; Garner, C. D.; Wever, R. *FEBS Lett.* **1988**, *235*, 93−97.

(45) Balhausen, C. J.; Gray, H. B. *Inorg. Chem.* **1962**, *1*, 111−122.

(46) Petersen, J.; Hawkes, T. R.; Lowe, D. J. *J. Am. Chem. Soc.* **1998**, *120*, 10978−10979.

(47) Tipton, P. A.; McCracken, J.; Cornelius, J. B.; Peisach, J. *Biochemistry* **1989**, *28*, 5720−5728.

(48) Calviou, L. J.; Collison, D.; Garner, C. D.; Mabbs, F. E.; Passand, M. A.; Pearson, M. *Polyhedral* **1989**, *8*, 1835−1837.

(49) Gerfen, G. J.; Hanna, P. A.; Chasteen, N. D.; Singel, D. J. *J. Am. Chem. Soc.* **1991**, *113*, 9513−9519.